Original Article
Effect of ultrasonic irradiation intensity on EGFP gene transfection and expression in tissue between bone defects in rabbits by ultrasound-mediated microbubble destruction

Shiwei Li[1], Xiaoli Xie[2], Xueyang Tang[1], Lijun Liu[1], Fang Liu[3]

[1]Department of Pediatric Surgery, West China Hospital, Sichuan University, Chengdu, Sichuan Province, P. R. China; [2]Department of Pediatric Surgery, Guangzhou Women and Children's Medical Center, Guangzhou, Guangdong Province, P. R. China; [3]Department of General Surgery, The First People's Hospital of Longquanyi District, Chengdu, Sichuan Province, P. R. China

Abstract: Purpose: To investigate the effect of different ultrasound intensities on enhanced green fluorescence protein (EGFP) gene expression in tissue between bone defects by ultrasound-mediated microbubble destruction (UMMD) and to evaluate the tissue damage after transfer. Method: Thirty rabbits were randomly divided into six groups: A1, A2, A3, A4, A5 and A6 (six in each group of A1-A4, and three in each group of A5-A6). Bone defect models were generated on the right ulnas. On the 10th day after model generation, suspension of EGFP plasmids and microbubbles (PM, 0.3 ml/kg) was locally injected to groups A1-A4, while plasmid-saline (PS, 0.3 ml/kg) was locally injected to groups A5 and A6. Then, ultrasound was given to the 6 groups at 0.5 W/cm^2, 1.0 W/cm^2, 1.5 W/cm^2, 2.0 W/cm^2, 1.0 W/cm^2, and 0 W/cm^2, respectively, with all other parameters remaining constant. Two rabbits were sacrificed for sample harvesting on the 3rd day, 7th day, and 14th day after gene transfer in groups A1-A4, and all rabbits were sacrificed on the 7th day after gene transfer in groups A5 and A6. The EGFP expression was quantified by average optical density under a fluorescence microscope. Tissue damage was observed under an optical microscope and an electron microscope. Results: On the 3rd day after transfection, groups A1 and A2 both had higher AOD ($P<0.05$) when compared to the others. However, there was no significant difference between these two groups ($P>0.05$). On the 7th day after transfection, AOD was significantly higher in groups A1-A4 than that in A5 and A6 ($P<0.05$), among which, groups A1 and A2 were the groups with the highest AOD ($P<0.05$). On the 14th day after transfection, there was no significant difference in AOD measurement among all groups ($P>0.05$). Tissue damage was detected under an optical microscope and an electron microscope in all groups at all observation points. A correlation between the severity of tissue damage and the intensity of experimental ultrasound was observed. Conclusions: EGFP gene can be efficiently transfected without obvious toxicity in bone defects of rabbits at 0.5 W/cm^2, when other parameters were set as follows: frequency: 1 MHz, duty ratio: 20%, and exposure duration: 1 min.

Keywords: Bone defects, microbubble, ultrasound, gene transfer, enhanced green fluorescence protein

Introduction

Reconstruction of bone defects caused by trauma, tumor resection, and infection remains a therapeutic problem in the orthopedic field [1-4], which brings not only long-term pain and disability to the patients but also extra financial burdens to their families, as well as the whole community. Traditional therapies, such as autologous bone grafts, allogenous bone grafts, and Ilizarov bone transport techniques

all have their own drawbacks, including complications on the donor site, extra surgical procedures, limitation in volume, uncontrollable graft resorption, potential immune rejection, and prolonged period of rehabilitation [3, 5-7].

It is very important to identify the mechanism of stimulating endogenous osteogenesis. Bone morphogenetic proteins (BMPs) are believed to be the most powerful growth factors that can induce the osteogenic differentiation of mesen-

chymal cells [8]. However, most growth factors have short half-life periods and tend to gradually disappear from the site of injury [9]. With the advances in molecular biology, gene therapy has been introduced to orthopedic study. Related research has shown that BMP-2 gene therapy can promote the healing process of bone defects [4, 10].

Transfer technique is one of the key points in gene therapy. Adenoviral vector has been proved to be the more efficient method, but concerns over potential toxicity and immunogenicity have hampered its clinical application [9, 11]. Non-viral methods are safer, but they are limited in terms of transfection efficiencies [9, 12]. In recent years, research has shown that ultrasound-mediated microbubble destruction (UMMD) within the safe range of frequency, time and intensity can improve the efficiency of trans-membrane gene transfer. The sonoporation created by ultrasound exposure can reversibly increase the permeability to the plasmid of the cell membrane. Furthermore, microbubbles, an ultrasonography contrast agent, can create a cavitation with the presence of ultrasound, which results in a bursting of the microbubbles, leading to a distribution of the plasmid over a specific area of interest [13]. Compared to other transfer approaches, UMMD is safe and efficient and can be easily repeated [9, 12]. Although genes have been successfully transferred into various cells and tissues in vivo and in vitro by this novel method, UMMD has its own shortcomings. The transfer efficiency by UMMD is not only affected by the properties of microbubbles but also related to ultrasound parameters [9]. The optimal ultrasound parameters differ among different tissue types and organs. It is difficult to apply the research findings in a specific domain to another. Previous studies have applied the UMMD transfer approach into the field of orthopedics [9, 14-17], but no application to bone defect in vivo has been reported yet. Ultrasound parameters, including the intensity, time, and duty ratio, have a critical effect on the efficiency of gene transfer and expression. Inappropriate parameters may not only reduce the efficiency but also induce serious tissue damage [13, 18, 19].

In this study, we applied UMMD as a gene transfer approach to bone defects in rabbit models. We aimed to examine the optimal ultrasonic irradiation intensity for EGFP gene trans-

fer in tissue between bone defects of rabbits with given parameters.

Materials and methods

Animals

Thirty 3-month-old male New Zealand rabbits weighing 2.5±0.5 kg were purchased from the Animal Experimental Center of Sichuan University. Rabbits were fed with standard laboratory chow and water in a standard animal room with appropriate temperature and humidity. All animal procedures were performed under the guidance of the Ethics Committee of West China Hospital of Sichuan University.

Reagents

Plasmid encoding EGFP was purchased from Tianmo Company (Beijing, China), and the concentration of plasmid was 1 mg/ml. SonoVue microbubbles were purchased from BRACCO (Milan, Italy). SonoVue containing a sulphur hexafluoride (SF_6) gas was encapsulated by a phospholipid shell and had a mean diameter of 2.5 pm. Penicillin was purchased from United Laboratories (Hong Kong, China).

Bone defect model

Rabbits were randomly divided into six groups (A1: 0.5 W/cm^2+PM (EGFP plasmids and microbubbles), A2: 1.0 W/cm^2+PM, A3: 1.5 W/cm^2+PM, A4: 2.0 W/cm^2+PM, A5: 1.0 W/cm^2+PS (plasmid-saline), and A6: 0 W/cm^2+PS), with six in each group for groups A1-A4 and three in each group for groups A5 and A6. Rabbits were sedated by 3% pentobarbital sodium (40 mg/kg) through an ear vein injection. Hair on the right forelimbs was shaved after the animals were fixed on the experimental plate. With prone positioning, the rabbits were sterilized and incised to expose the middle section of the right ulna, and bone defects of 2.0 cm in length were created. Then, incisions were sutured layer by layer. Penicillin of 400000 u was used through intramuscular injection at 30 minutes pre-surgery, as well as 24 and 48 hours post-surgery to prevent infection. After being awakened, the rabbits were fed normally.

Preparation of plasmids and microbubbles suspension

SonoVue was dissolved in 5 ml of saline and was vibrated to be thoroughly mixed. Then, the

plasmid and dissolved SonoVue were mixed in a volume ratio of 1:2. The suspension was incubated at room temperature for 30 minutes and was preserved in a 4°C refrigerator.

EGFP gene transfer

On the 10th day after model generation, suspension of PM (0.3 ml/kg) was injected to bone defect sites with a 5-mm depth of needle insertion in groups A1-A4 while PS was injected in groups A5 and A6 with the same dosage and injection pathway. Ultrasound was generated from an ultrasound therapy device (Sonic Master ES-2, OG Giken, Okayama, Japan) immediately. The probe frequency was set at 1 MHz, and the probe area was 10 cm^2. The skin at bone defect sites was spread with coupling gel. Ultrasound was performed at 1 MHz, duty ratio of 20% for 1 minute at the surface of the target area immediately, and ultrasonic intensity was set at 0.5 W/cm^2, 1.0 W/cm^2, 1.5 W/cm^2, 2.0 W/cm^2, 1.0 W/cm^2, and 0.0 W/cm^2, respectively.

Histological analysis

In groups A1-A4, two rabbits in each group were sacrificed with an overdose of pentobarbital sodium on the 3rd day, 7th day and 14th day after transfer. In groups A5 and A6, all rabbits were sacrificed on the 7th day after transfer. Two soft-tissue samples with a size of approximately 0.5 cm*0.5 cm*0.5 cm were harvested from the bone defect site of each rabbit, one for frozen section and the other for transmission electron section.

For cryosection preparation, soft tissue was placed immediately in a frozen microtome for 15 mins and trimmed and embedded, then 4,6-diamidino-2-phenylindole nuclear counterstains were performed. Longitudinal sections were sliced as thin as 20-μm to 40-μm intervals. Two frozen sections were stained with Dapi and one was stained with H&E. Dapi-stained sections were observed under a fluorescence microscope (LEICA DFC495, Germany) with 200× magnification field of view. Images of five typical points expressing green fluorescence protein in each frozen section were captured for semi-quantitative analyses using pathological image analysis software (Image-Pro Plus 6.0, Media Cybernetics, USA). The data were expressed as average optical density (AOD).

For H&E staining, the tissues were cut in a frozen microtome into 5-μm slices and stained with H&E to observe the damage to the tissue under a general microscope (OLYMPUS DP70, Japan).

For transmission electron section, samples were fixed in 4% p-formaldehyde and 1% glutaraldehyde in 0.1 M phosphate buffer (pH 7.2) for 48 h. The specimens were post-fixed in 2% osmium tetroxide for 1 h (Electron Microscopy Science, Hatfield, PA) and dehydrated in a graded series of ethanol solutions (from 50% to 100%) and propylene oxide. The samples were then embedded in epoxy resin LX 112 (SIGMA-Aldrich) and incubated for 24 h at 37°C, and the resin was polymerized for 48 h at 60°C. Sixty-nanometer sections were cut transversely using an Ultracut UCT ultramicrotome (Leica) with respect to the main axis of collagen fibers, stained with 5% uranyl acetate, and placed on electron microscopy one-slot grids coated with Formvar film. The sections were then observed at 100 kV with a Jeol 1011 transmission electron microscope (JEOL Ltd., Tokyo, Japan) connected to a Gatan digital camera driven by Digital Micrograph software (Gatan, Pleasanton, CA).

Statistical analysis

Data are presented as the mean ± SD. Differences among groups were evaluated with one-way analysis of variance, and LSDs or Tamhane-tests were used between two groups at the same time point. Differences among different time points were evaluated with one-way analysis of variance, LSDs were used between different time points in the same group. The significance was defined as a *p*-value <0.05. SPSS16.0 statistical analysis software (SPSS, Chicago, IL, USA) was used for data analysis.
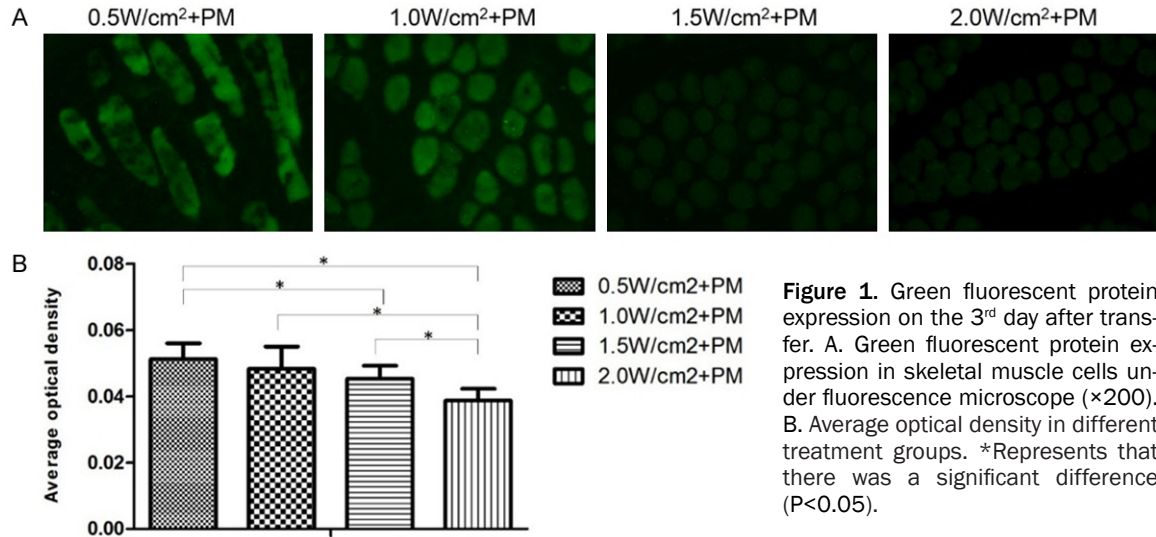
Results

General state of rabbits

The general conditions were good in all animals, and there were no rabbit deaths. The wounds were free of inflammation, suppuration and exudation after surgery in all periods.

Local changes in gross samples

The tissue around the bone defect was pale yellow in color. Hyperemia and swelling of tissue

Figure 1. Green fluorescent protein expression on the 3rd day after transfer. A. Green fluorescent protein expression in skeletal muscle cells under fluorescence microscope (×200). B. Average optical density in different treatment groups. *Represents that there was a significant difference (P<0.05).

was detected. Many blood clots were observed between the broken ends of the bone defect.

Green fluorescent protein expression of different groups within the same period

On the 3rd day after transfer, green fluorescence was detected in groups A1-A4. Green fluorescent protein expression was found in skeletal muscle cells, fibroblasts, vascular endothelial cells, cartilage tissue and nerve tissue, among which the skeletal muscle cells had the strongest expression. Overall, the AOD of green fluorescence declined with increasing ultrasound intensity (**Figure 1A**). Groups A1 and A2 had higher AOD (P<0.05) when compared to other groups, but there was no significant difference between these two groups (P>0.05) (**Figure 1B**). On the 7th day after transfer, all groups had green fluorescence expression (**Figure 2A**), and there was a downtrend of AOD with the increase of ultrasound intensity in groups A1-A4 (**Figure 2B**). Similarly, groups A1 and A2 had higher AOD (P<0.05), while there was no significant difference (P>0.05) between the two. Groups A5 and A6 had lower AOD (P<0.05) when compared to the other four groups. On the 14th day after transfer, green fluorescence expression can still be found in all groups (**Figure 3A**), but there was no difference in AOD among all groups (P>0.05) (**Figure 3B**).

Green fluorescent protein expression of different period in the same group

Gene expression gradually increased in groups A1 and A2 over time, and a significant difference between day 3 and day 14 was detected

(P<0.05) (**Figure 4A**, **4B**). While the AOD was on the decline between both the 3rd and 7th day after transfer, which then rose again between the 7th and 14th day after transfer in groups A3 and A4, and there was a significant difference in AOD among different interested time points (P<0.05) (**Figure 4C**, **4D**).

Tissue damage under optical microscope

On the 3rd day after transfer, soft tissue edema and a small amount of neutrophil infiltration were detected in group A1. Signs of necrosis such as cytolysis, karyorrhexis and phagocytosis of inflammatory cells were not seen. In group A2, the tissue edema was much more severe. The number of inflammatory cells increased and very few muscle cells were being swallowed by inflammatory cells. In group A3, muscle cell necrosis was also detected. In group A4, tissue edema aggravated and partial muscle cells lysed. At the same time, there was desmoplasia around muscle bundles (**Figure 5A**). Tissue damage reduced in all groups on the 7th day after transfer, and tissue was almost completely repaired on the 14th day after transfer (**Figure 5B** and **5C**).

Damage of muscle cells under transmission electron microscope

On the 3rd day after transfer, swelling of muscle cells and vacuole degeneration were detected in groups A1-A3. The mitochondria and sarcoplasmic reticulum in some muscle cells were apparently swelling in group A3. In group A4, signs of necrosis, such as cytolysis and karyor-
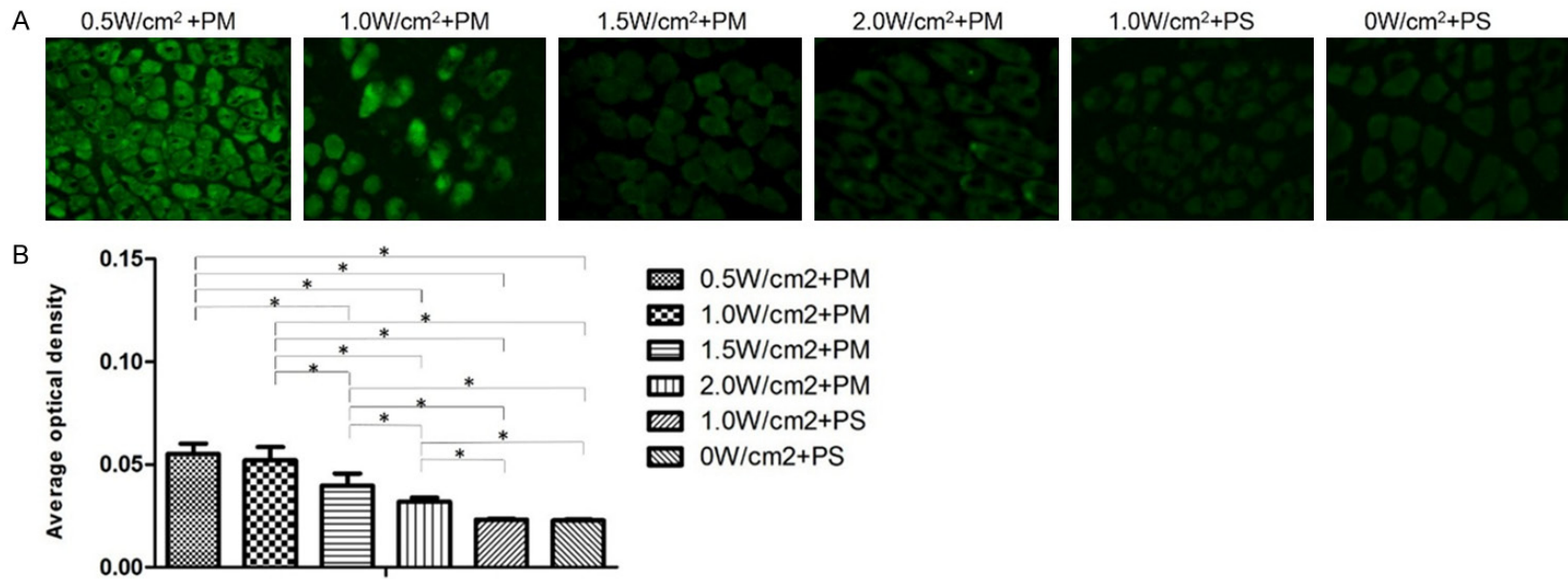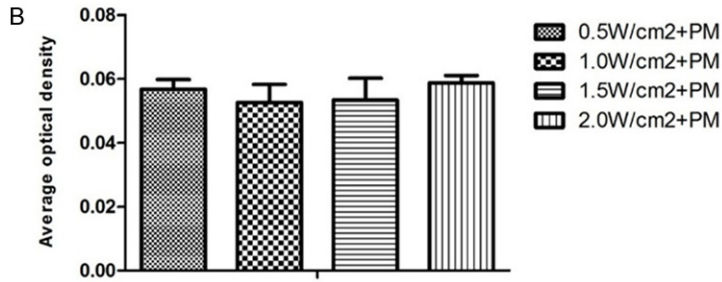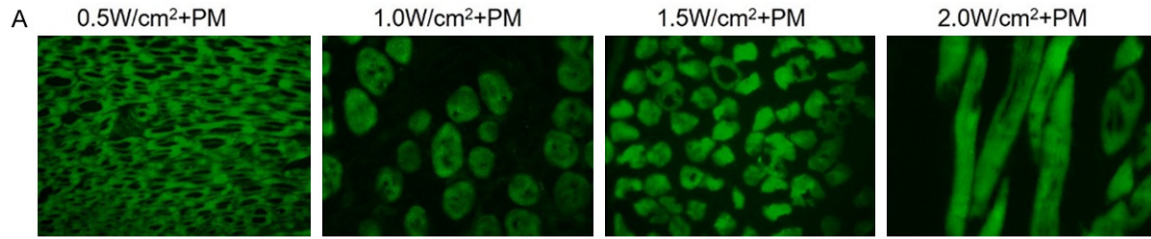
Figure 2. Green fluorescent protein expression on the 7th day after transfer. A. Green fluorescent protein expression in skeletal muscle cells under a fluorescence microscope (×200). B. Average optical density in different treatment groups. *Represents that there was a significant difference ($P<0.05$).

Figure 3. Green fluorescent protein expression on the 14th day after transfer. A. Green fluorescent protein expression in skeletal muscle cells under fluorescence microscope (×200). B. Average optical density in different treatment groups.
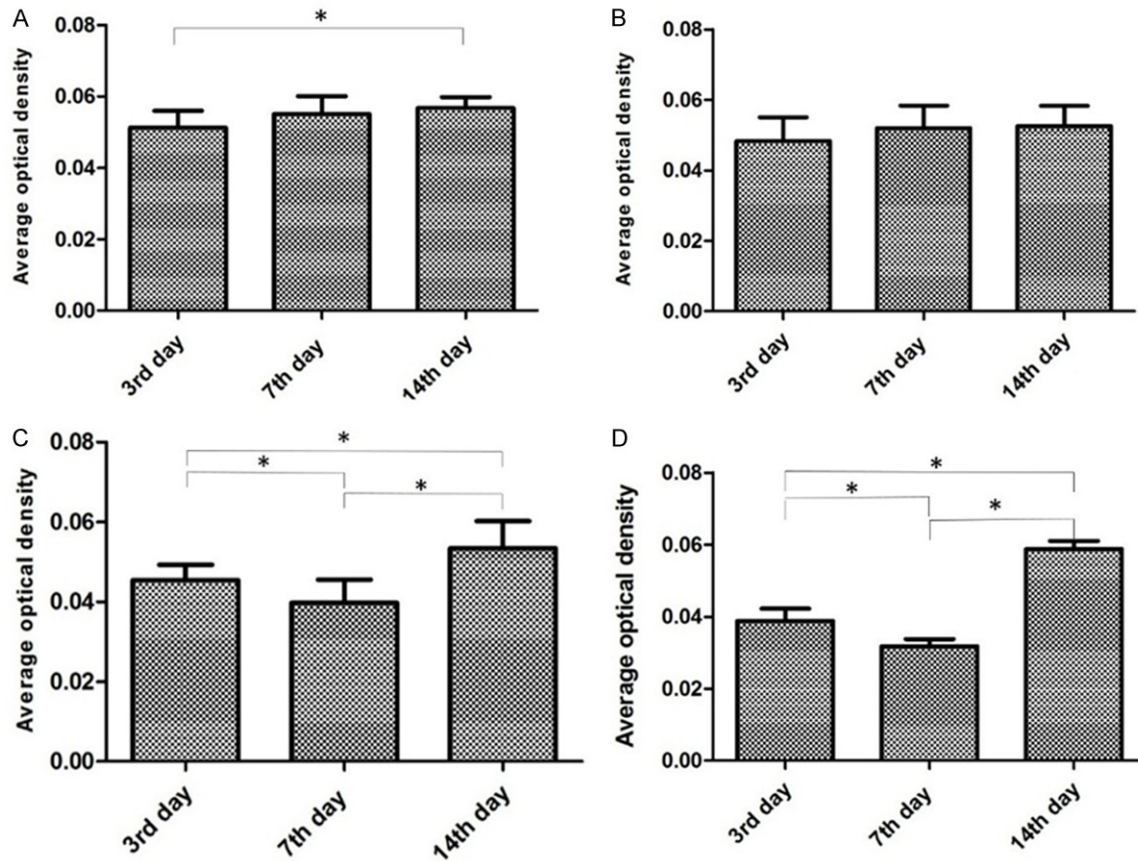
**Figure 4.** Average optical density of different periods in the same group. (A) 0.5 W/cm^2+PM. (B) 1.0 W/cm^2+PM. (C) 1.5 W/cm^2+PM, and (D) 2.0 W/cm^2+PM. *Represents that there was a significant difference (P<0.05).

rhexis were detected. The myofilaments had an irregular arrangement, and the gaps among myofilaments were broadened (**Figure 6A**). Damage of muscle cells was reduced on the 7th day after transfer (**Figure 7A**).

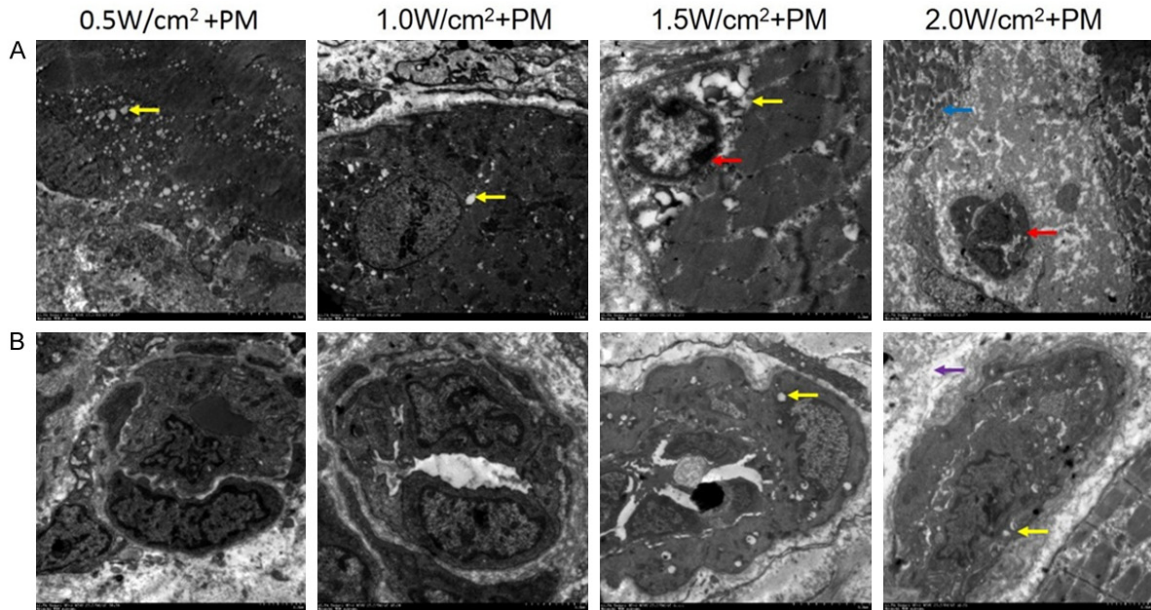*Damage of vascular endothelial cells under transmission electron microscope*

On the 3rd day after transfer, vascular endothelial cells were activated with formal cell connec-
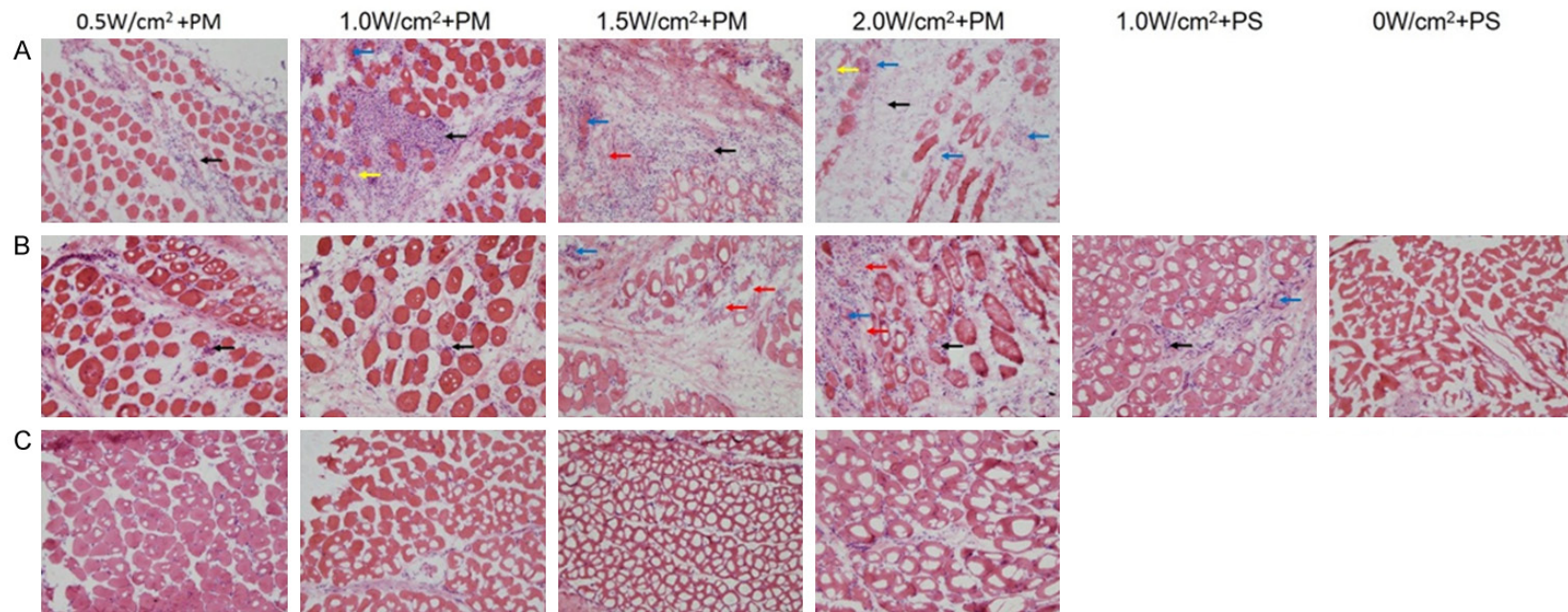
Figure 5. Tissue damage under an optical microscope at different times (×200). A. The 3rd day after transfer. B. The 7th day after transfer. C. The 14th day after transfer. The black arrow indicates neutrophils infiltration. The yellow arrow indicates the lysed muscle cells. The blue arrow indicates muscle cells swallowed by inflammatory cells. The red arrow indicates the necrosis of muscle cells.

Figure 6. Tissue damage under a transmission electron microscope on the 3rd day after transfer. A. Muscle cells. B. Vascular endothelial cells. The yellow arrow indicates vacuole degeneration. The red arrow indicates karyorrhexis. The blue arrow indicates disorganized myofilaments. The purple arrow indicates non-structural area.

tion in groups A1 and A2. The Endoplasmic reticulum was activated and no evidence was found to reveal cell necrosis. Swelling of mitochondria and vacuoles in cytoplasm was discovered in groups A3 and A4. In group A4, a large area of non-structural area around the endothelial cells was detected (**Figure 6B**). Damage of vascular endothelial cells was reduced on the 7th day after transfer (**Figure 7B**).

Discussion

Many previous studies have shown that UMMD can successfully transfect genes into various tissues and cells both in vivo and in vitro. Gene transfer mediated by UMMD has been demonstrated in the heart, liver, blood vessels, kidney, and skeletal muscle [13, 20-24]. Nonetheless, there is reportedly no study that examines the application of this novel gene transfer method in bone defects. Inappropriate ultrasonic parameters, especially the critical ones such as irradiation intensity, can not only reduce the transfection efficiency but also lead to side effects such as tissue damage.

Observing green fluorescent protein expression on the 3rd day and 7th day after transfer, our experiments showed that under the same mechanical indexes, duty ratio and irradiation time, the gene expression efficiency decreased upon the increase of the ultrasound intensity. When intensity of ultrasound was set at 0.5 W/cm^2, the soft tissue expressed the strongest green fluorescence, followed by 1.0 W/cm^2, 1.5 W/cm^2 and 2.0 W/cm^2 on the 3rd day and 7th day after transfer. However, there was no significant difference between the 0.5 W/cm^2 group and the 1.0 W/cm^2 group. The reason, combined with the optical microscope and transmission electron microscope results, may be that strong ultrasound irradiation induced soft tissue edema, cell damage and inflammatory at bone defect sites, which directly affect the successful transfection and expression of the target gene.

On the 14th day after transfer, the cells have mostly finished their self-repair with the resolution of inflammation; hence, the target cells transfected with different ultrasound intensities can fully express EGFP. Thus, groups with different irradiation intensities had no differences in EGFP expression on the 14th day after gene transfer.

In low irradiation intensity groups (0.5 W/cm^2 and 1.0 W/cm^2), the EGFP expression increased with time. EGFP expression may be related to the condition of the target cells. In this study,
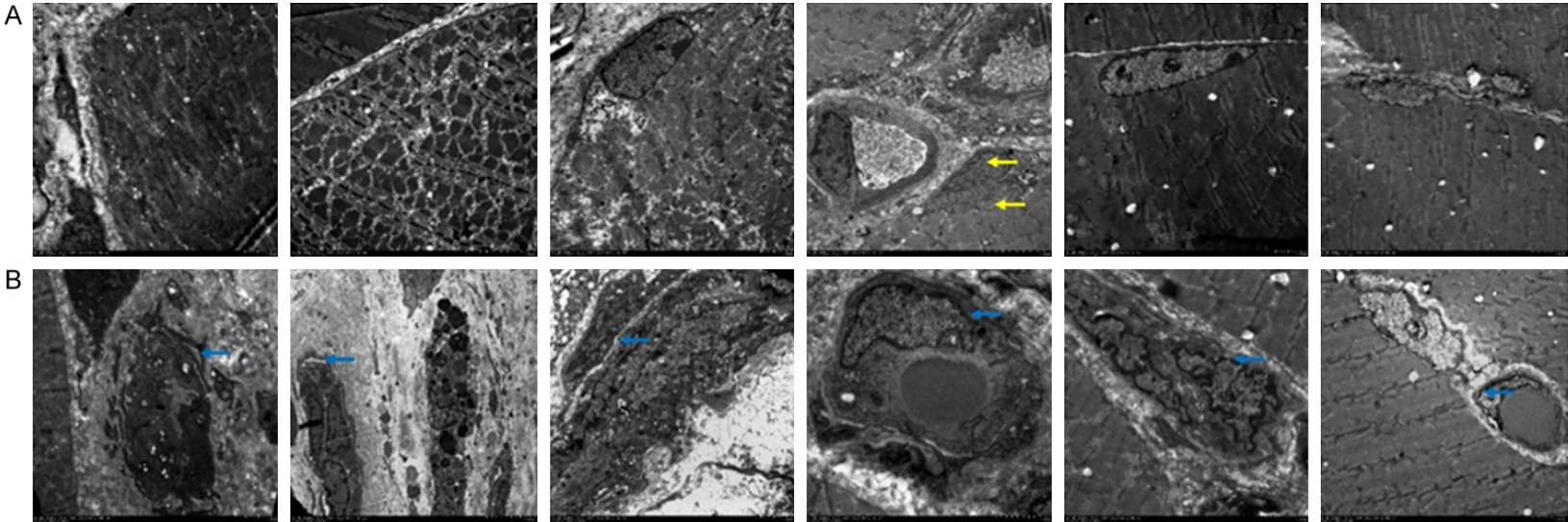
Figure 7. Tissue damage under transmission electron microscope on the 7th day after transfer. A. Muscle cells. B. Vascular endothelial cells. The yellow arrow indicates mitochondria swelling. The blue arrow indicates vascular endothelial cells.

alleviation of the tissue edema and cell damage shown by light microscope and electron microscope aligned with the tissue self-repair process over time. It seems that the ability to express EGFP may gradually increase with the self-repair of cells and the resolution of inflammation, although the increase may be subtle. The fact that no significant differences were found among some different time points may be caused by insufficient animals or short observation intervals.

In higher irradiation intensity groups (1.5 W/cm^2 and 2.0 W/cm^2), strongest EGFP expression was detected on the 14th day after transfer, followed by the 3rd day and the 7th day. Our hypothesis is that there was some edema, but live targeted cells did not lose their function of gene expression on the 3rd day after higher intensity of ultrasound irradiation. However, since some edema cells could not self-repair and eventually die a weaker fluorescence intensity will be seen on the 7th day after transfer. On the 14th day after transfer, the strongest fluorescence observed was caused by the enhancement of tissue recovery and cell proliferation.

UMMD could enhance EGFP expression in multiple types of cells at bone defect sites according to these study results. Although the EGFP expression is untargeted transfection and the expression intensity among different cells are different, the underlying mechanism remains unclear. It is suspected that non-targeted microbubbles used in this study and different responses to ultrasound energy for different cells should be jointly responsible for the above findings. It is also suspected PM concentrations were not the same in different areas of the bone defect site around local injection. All kinds of cells may receive EGFP gene by UMMD, when microbubbles were destructed by ultrasound irradiation. Consequently, multiple kinds of cells will express EGFP eventually. Because skeletal muscle cells were bigger in size than other cells, they may get to absorb more PM. Therefore, a stronger expression of EGFP can be detected in muscle cells. One of the other reasons may be related to the fact that skeletal muscle cells are located in the superficial layer while other cells were located in deeper levels in bone defect areas. Skeletal muscle cells could receive more gene plasmids than other cells in deeper layers because ultrasonic energy decays with the increase of distance. This non-targeted gene transfer technology may arguably have some potential risks and may reduce efficiency of transfection. Therefore, targeted microbubbles for specific cells in bone defects should be invented in the future as in other organs [25, 26].

Conclusion

UMMD can promote EGFP gene transfection and expression at the bone defect site in rabbits. Moreover, 0.5 W/cm^2 ultrasound intensity can achieve higher efficiency of gene transfection with mild tissue damage under the same condition. Ultrasonic irradiation intensity of 0.5 W/cm^2 is appropriate in the future UTMD experiments for rabbit bone defection.

Acknowledgements

Disclosure of conflict of interest

None.

Address correspondence to: Dr. Xueyang Tang, Department of Pediatric Surgery, West China Hospital, Sichuan University, 37 Guo Xue Road, Chengdu 610041, Sichuan Province, P. R. China. Tel: +8602-885422456; E-mail: tangxueyang100@163.com

References

[1] Karger C, Kishi T, Schneider L, Fitoussi F, Masquelet AC; French Society of Orthopaedic Surgery and Traumatology (SoFCOT). Treatment of posttraumatic bone defects by the induced membrane technique. Orthop Traumatol Surg Res 2012; 98: 97-102.

[2] Wiese A and Pape HC. Bone defects caused by high-energy injuries, bone loss, infected nonunions, and nonunions. Orthop Clin North Am 2010; 41: 1-4.

[3] Wang Y, Van Manh N, Wang H, Zhong X, Zhang X and Li C. Synergistic intrafibrillar/extrafibrillar mineralization of collagen scaffolds based on a biomimetic strategy to promote the regeneration of bone defects. Int J Nanomedicine 2016; 11: 2053-2067.

[4] Kolk A, Tischer T, Koch C, Vogt S, Haller B, Smeets R, Kreutzer K, Plank C and Bissinger O. A novel nonviral gene delivery tool of BMP-2 for the reconstitution of critical-size bone defects in rats. J Biomed Mater Res A 2016; 104: 2441-2455.

[5] Younger EM and Chapman MW. Morbidity at bone graft donor sites. J Orthop Trauma 1989; 3: 192-195.

[6] Hertel R, Gerber A, Schlegel U, Cordey J, Rüegsegger P, Rahn BA. Cancellous bone graft for skeletal reconstruction. Muscular versus periosteal bed--preliminary report. Injury 1994; 25 Suppl 1: A59-70.

[7] Van der Stok J, Van der Jagt OP, Amin Yavari S, De Haas MF, Waarsing JH, Jahr H, Van Lieshout EM, Patka P, Verhaar JA, Zadpoor AA and Weinans H. Selective laser melting-produced porous titanium scaffolds regenerate bone in critical size cortical bone defects. J Orthop Res 2013; 31: 792-799.

[8] Smeets R, Maciejewski O, Gerressen M, Spiekermann H, Hanisch O, Riediger D, Blake F, Stein J, Holzle F and Kolk A. Impact of rh-BMP-2 on regeneration of buccal alveolar defects during the osseointegration of transgingival inserted implants. Oral Surg Oral Med Oral Pathol Oral Radiol Endod 2009; 108: e3-e12.

[9] Qiu L, Zhang L, Wang L, Jiang Y, Luo Y, Peng Y and Lin L. Ultrasound-targeted microbubble destruction enhances naked plasmid DNA transfection in rabbit achilles tendons in vivo. Gene Ther 2012; 19: 703-710.

[10] Betz OB, Betz VM, Schröder C, Penzkofer R, Göttlinger M, Mayerwagner S, Augat P, Jansson V and Müller PE. Repair of large segmental bone defects: BMP-2 gene activated muscle grafts vs. autologous bone grafting. BMC Biotechnol 2013; 13: 1-9.

[11] Nishida K, Doita M, Takada T, Kakutani K, Miyamoto H, Shimomura T, Maeno K and Kurosaka M. Sustained transgene expression in intervertebral disc cells in vivo mediated by microbubble-enhanced ultrasound gene therapy. Spine (Phila Pa 1976) 2006; 31: 1415-1419.

[12] Osawa K, Okubo Y, Nakao K, Koyama N and Bessho K. Osteoinduction by microbubble-enhanced transcutaneous sonoporation of human bone morphogenetic protein-2. J Gene Med 2009; 11: 633.

[13] Chen ZY, Yang F, Lin Y, Zhang JS, Qiu RX, Jiang L, Zhou XX and Yu JX. New development and application of ultrasound targeted microbubble destruction in gene therapy and drug delivery. Current Gene Therapy 2013; 13: 250.

[14] Li P, Gao Y, Liu Z, Tan K, Zuo Z, Xia H, Yang D, Zhang Y and Lu D. DNA transfection of bone marrow stromal cells using microbubble-mediated ultrasound and polyethylenimine: an in vitro study. Cell Biochem Biophys 2013; 66: 775.

[15] Inoue H, Arai Y, Kishida T, Shinya M, Terauchi R, Nakagawa S, Saito M, Tsuchida S, Inoue A and Shirai T. Sonoporation-mediated transduction of siRNA ameliorated experimental arthritis using 3 MHz pulsed ultrasound. Ultrasonics 2014; 54: 874-881.

[16] Delalande A, Bouakaz A, Renault G, Tabareau F, Kotopoulis S, Midoux P, Arbeille B, Uzbekov R, Chakravarti S, Postema M and Pichon C. Ultrasound and microbubble-assisted gene delivery in achilles tendons: long lasting gene expression and restoration of fibromodulin KO phenotype. J Control Release 2011; 156: 223-230.

[17] Qiu L, Jiang Y, Zhang L, Wang L and Luo Y. Ablation of synovial pannus using microbubble-mediated ultrasonic cavitation in antigen-induced arthritis in rabbits. Rheumatol Int 2012; 32: 3813-3821.

[18] Liang HD, Lu QL, Xue SA, Halliwell M, Kodama T, Cosgrove DO, Stauss HJ, Partridge TA and Blomley MJ. Optimisation of ultrasound-mediated gene transfer (sonoporation) in skeletal muscle cells. Ultrasound Med Biol 2004; 30: 1523.

[19] Koch S, Pohl P, Cobet U and Rainov NG. Ultrasound enhancement of liposome-mediated cell transfection is caused by cavitation effects. Ultrasound Med Biol 2000; 26: 897-903.

[20] Song S, Shen Z, Chen L, Brayman AA and Miao CH. Explorations of high-intensity therapeutic ultrasound and microbubble-mediated gene delivery in mouse liver. Gene Ther 2011; 18: 1006-1014.

[21] Fujii H, Li SH, Wu J, Miyagi Y, Yau TM, Rakowski H, Egashira K, Guo J, Weisel RD and Li RK. Repeated and targeted transfer of angiogenic plasmids into the infarcted rat heart via ultrasound targeted microbubble destruction enhances cardiac repair. Eur Heart J 2011; 32: 2075-2084.

[22] Phillips LC, Klibanov AL, Wamhoff BR and Hossack JA. Targeted gene transfection from microbubbles into vascular smooth muscle cells using focused, ultrasound-mediated delivery. Ultrasound Med Biol 2010; 36: 1470-1480.

[23] Ka SM, Yeh YC, Huang XR, Chao TK, Hung YJ, Yu CP, Lin TJ, Wu CC, Lan HY and Chen A. Kidney-targeting Smad7 gene transfer inhibits renal TGF-β/MAD homologue (SMAD) and nuclear factor κB (NF-κB) signalling pathways, and improves diabetic nephropathy in mice. Diabetologia 2012; 55: 509.

[24] Burke CW, Suk JS, Kim AJ, Hsiang YH, Klibanov AL, Hanes J and Price RJ. Markedly enhanced

skeletal muscle transfection achieved by the ultrasound-targeted delivery of non-viral gene nanocarriers with microbubbles. J Control Release 2012; 162: 414-421.

[25] Chang S, Guo J, Sun J, Zhu S, Yan Y, Zhu Y, Li M, Wang Z and Xu RX. Targeted microbubbles for ultrasound mediated gene transfection and apoptosis induction in ovarian cancer cells. Ultrason Sonochem 2013; 20: 171-179.

[26] Deshpande N, Lutz AM, Ren Y, Foygel K, Tian L, Schneider M, Pai R, Pasricha PJ and Willmann JK. Quantification and monitoring of inflammation in murine inflammatory bowel disease with targeted contrast-enhanced US. Radiology 2012; 262: 172-180.